SAND2016-10416R

Advanced high-spatial-resolution diffraction diagnostics

Paul G. Kotula (PI) and Mark H. Van Benthem
Sandia National Laboratories
Albuquerque, NM 87185

Abstract

Diffraction series data have been acquired and analyzed via multivariate statistical analysis. For two different data series analyzed, the data analysis was able to reduce the raw diffraction data series into a much smaller easier-to-interpret solution consisting mainly of crystallographic phase and orientation information.

Introduction

In materials characterization understanding the microstructure is important to reveal thermal history, anomalies, defects, aging, and failure modes. In addition to local chemical variations captured by characteristic X-rays in the transmission electron microscope for example, variation in crystal structure, orientation, and defects is captured by collecting diffraction patterns. Rather than collect patterns from just a few pre-chosen regions, newly developed methods allow us to collect full diffraction patterns from a series of points or pixels in an array so we can effectively sample the underlying crystallography, etc. in an unbiased way. Such diffraction series consist of a collection of full diffraction patterns acquired from a series of image points or pixels. The goal of this work is to capture as much information from the samples in a short time and post-process to reveal grains, orientations, phases and potentially defects. In principle, these contain a large amount of information about the phases, grains and respective orientations of the materials microstructure. Figure 1 shows the basic concept of diffraction imaging where the resulting image-resolved diffraction patterns have both real-space dimensions (30 x 30 pixels in the first example, 256 x 256 pixels in the second example) and reciprocal- or diffraction space dimensions (128 x 128 pixels and 264 by 264 pixels respectively). The challenge then is how to analyze such large diffraction series data sets. Amongst the variance we might expect is crystallographic phase, orientation, interfacial strain, magnetic domains, etc. A large part of the data's variance might also be

explained by redundancy. The goal of this ongoing work is to develop a method for efficient acquisition and analysis of diffraction series data sets to most efficiently and robustly acquire and analyze the resulting data to find what we perhaps expect as well as anomalies we might not otherwise be sensitive to.

Approach

The multivariate statistical analysis (MSA) data analysis methods we have applied to diffraction series are similar to those developed for analysis of hyperspectral X-ray data sets [1]. Early work on analyzing series of electron backscatter diffraction patterns [2] showed that in addition to orientation, close space groups (Fm3m versus Fd3m) and overlapped patterns could be separated. In this work we seek to

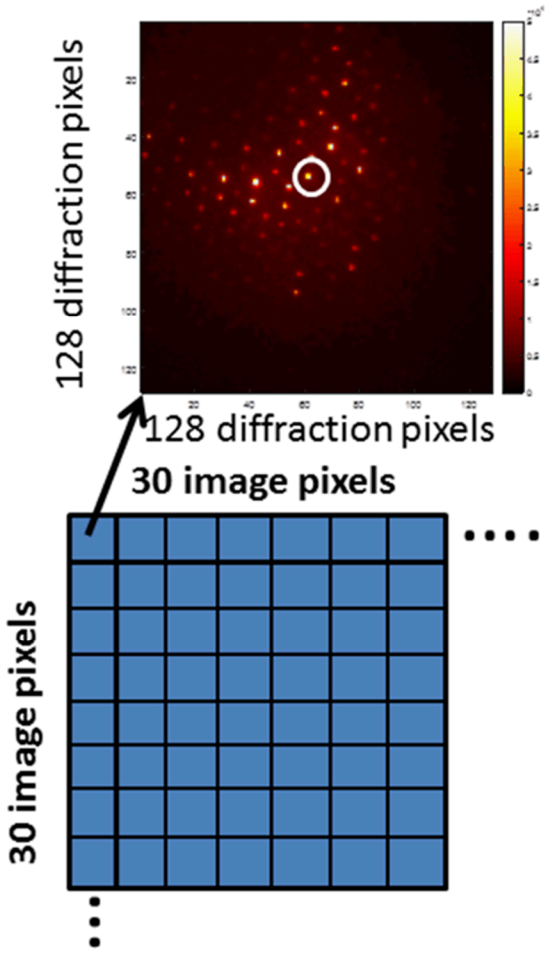

Figure 1. Schematic of a diffraction image where full diffraction patterns are acquired from an array of real-space pixels.

develop methods suited to the analysis of diffraction patterns from thin samples in the TEM to both improve spatial resolution and the number of grains through the thickness of a TEM foil. Schematically, Figure 2 shows the data analysis process and challenge. We start with 2D real-space pixels and 2D

diffraction-space pixels. For computational purposes, these both can be unfolded into vectors. As with other MSA methods, adjacency of real- or diffraction-space pixels does not matter unless we perform some type of binning. The specific MSA methods employed here follow a similar path as those developed for X-ray spectroscope data. Firstly we scale the data for noise, followed by factor analysis with the final step the inverse of the first, namely inverse noise scaling. The factor analysis step seeks to make the real-space factors simple or high-contrast [3] after the methods developed by Keenan. In Figure 2, D is the raw data scaled for noise, C is the real-space factors (like real-space images) and S is the reciprocal- or diffraction-space factors (like diffraction patterns). Implicit in this is that we have constructed a reduced (p) rank model of the data where $p << n, m$ where n are the number of unfolded diffraction pixels and m are the number of real-space pixels. In practice, we calculate the Eigenvalues of the scaled data and then examine the so-called scree plot (log eigenvalue versus sorted eigenvalue index) to look for obvious break points.

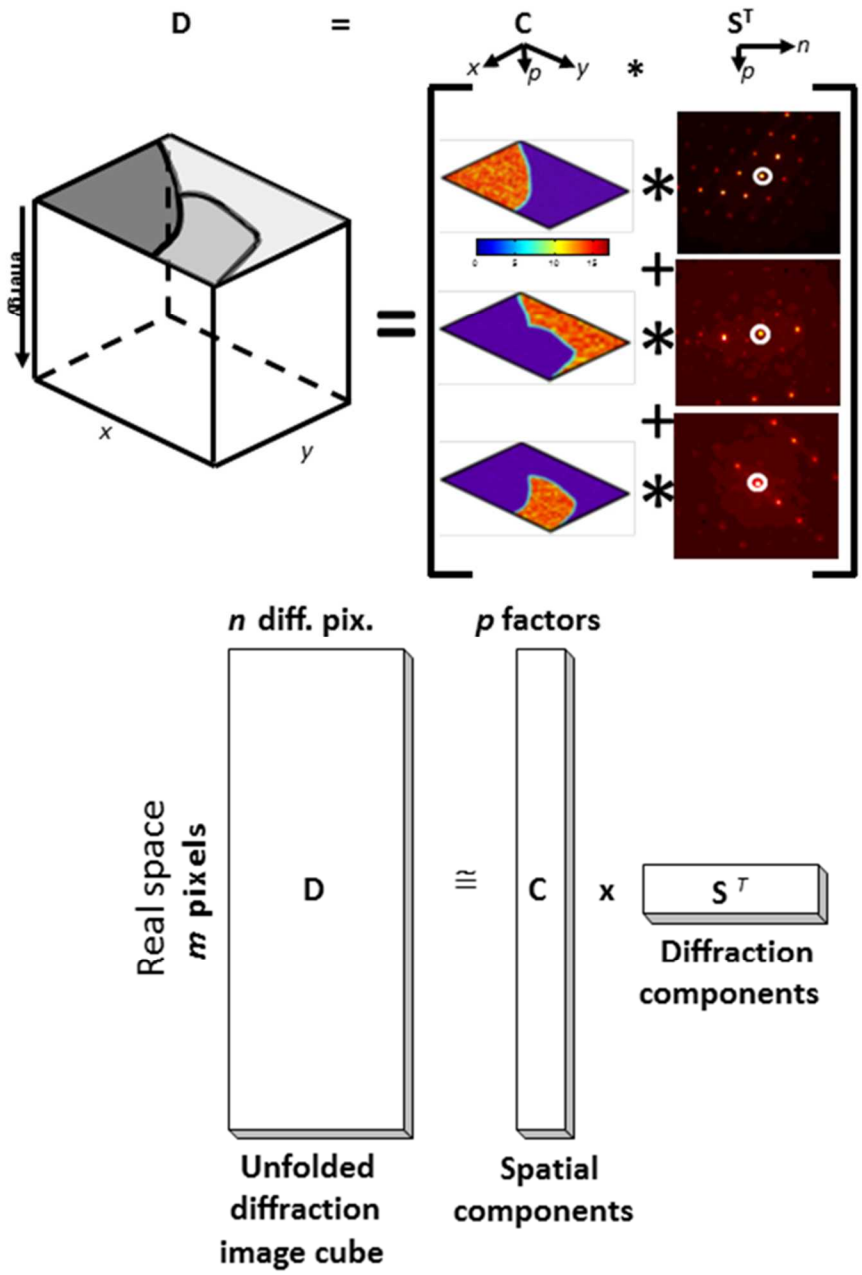

Figure 2. Schematic of the multivariate statistical analysis problem. 2D image pixels are unfoldedinto vectors as are the 2D diffraction patterns (below). For display purposes these are re-folded as shown in the top portion of the schematic.

Results and Impacts

In this limited study, we relied upon two previously acquired data sets. Firstly, position-resolved diffraction data were acquired on a FEI Company Titan 80-200 operated at 200kV and equipped with

three-condenser lenses and a probe spherical-aberration corrector. Parallel nano-beam diffraction (PND) patterns were acquired on a Gatan Orius 200D lens-coupled CCD and convergent-beam electron diffraction (CBED) patterns PNDetector direct electron camera [4]. PND data were acquired from a 30 by 30 real-space pixels each collected with a scanned 10 nm parallel nano-beam where each pattern consisted of 512 by 512 reciprocal-space pixels which were subsequently binned 4 by 4 to 128 by 128 pixels for a data set of 30 Mb. The CBED diffraction series consisted of 256 by 256 real-space pixels by 264 by 264 diffraction-space pixels with 20 replicates at each real-space pixels. This data set was 192 Gb and challenges the previous methods which were developed on data sets with one small dimension (typically the number of spectral channels).

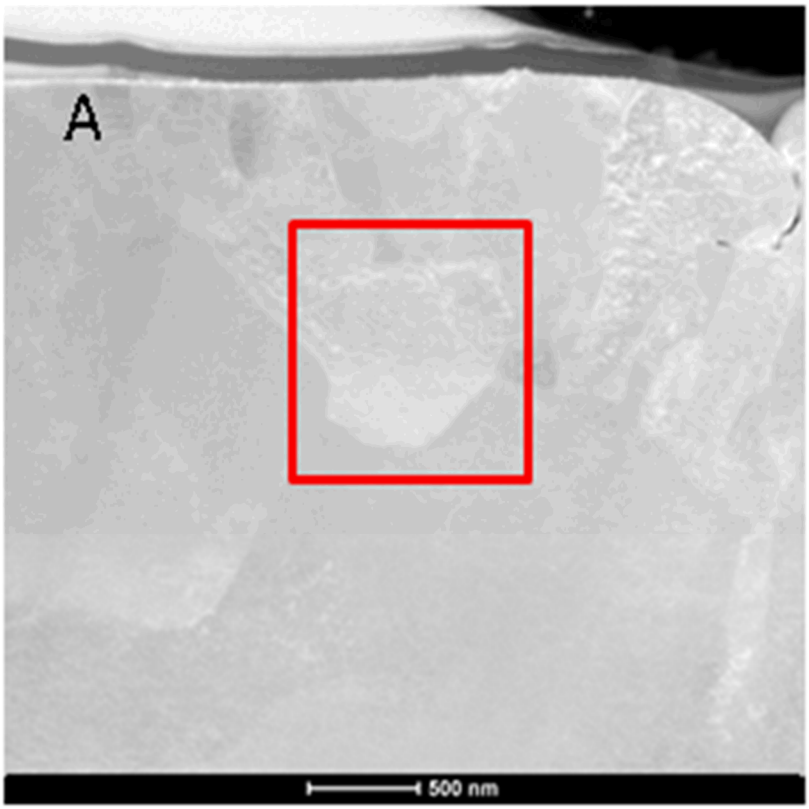

Figure 3. Cross-section high-angle annular dark-field STEM image of an electrical contact material (Paliney 7) which had been electro discharge machined (EDM). The inset red square shows the region where the PND data were acquired. The diffraction pattern in Figure 1 is a raw pattern from the PND data set.

Analysis with MSA of the PND data set showed a clear break-point in the scree plot at 9 factors and these show the grain structure quite clearly. If we specifically look at one pixel in Figure 4 (bottom experimental pattern), where two adjacent grains overlap through-thickness of the 100-nm thick TEM foil, we see a somewhat complicated pattern clearly arising from more than one grain.

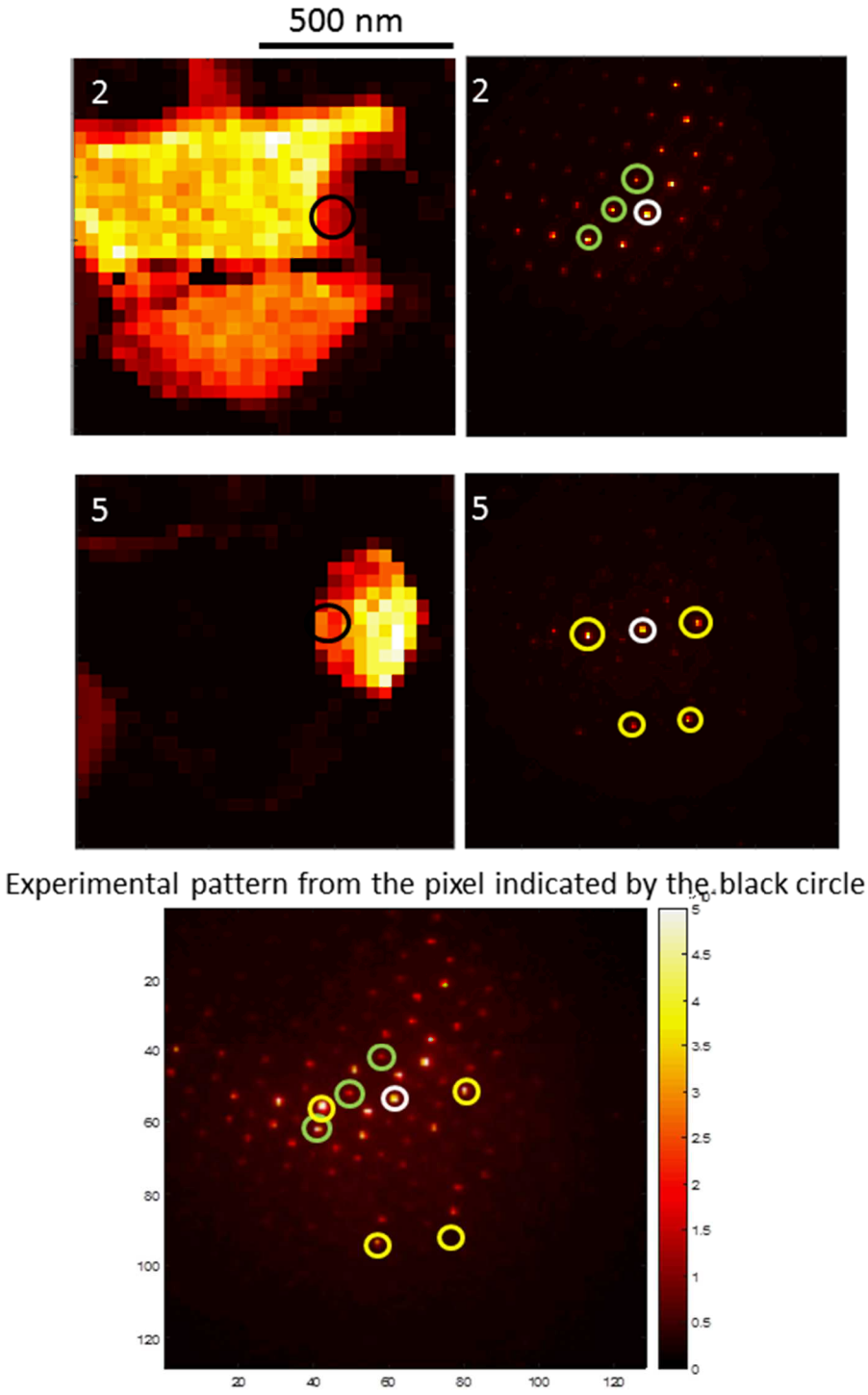

Figure 4. MSA results factors 2 and 5 which have an overlapped region indicated by the black circle. Bottom is the raw diffraction pattern from the black-circled spatial region. White circles in the diffraction patterns are the pattern center while the green (2) and yellow (5) allow the reader to follow some reflections. The MSA has successfully unmixed the experimental pattern to its underlying two 'pure' patterns.

In this MSA has successfully unmixed the overlapped region. The total of the 9-factor model shows the grain structure including mixed patterns. Conventional data analysis methods relying on pattern matching will find the best fit which might be neither of the two correct underlying orientations [5].

The CBED diffraction series, at 183 Gb, posed a much larger computational challenge. Here we scanned a converged beam at 3 nm/real-space pixel and acquired 20 replicate diffraction patterns per real-space pixel at 1 msec/pattern with a direct electron camera. With 20 replicates per pixel, we calculated the variance due to noise upon reading in all the data. Reading in the data and calculating the variance images took 93 minutes, calculating the covariance matrix took 13 minutes, the Eigenanalysis took 21 minutes and the factor rotation took 45 seconds. Fortunately much of this need only be done once and then stored as processed. Figure 5 shows a subset of the results. The specimen was acquired from the Arltunga meteorite from a region of ferrite and austenite. For the analysis at hand we calculated two models of the data, rank 8 and rank 45. Both are approximations and correspond to break-points in the scree plot. The rank 8 model showed both ferrite and austenite of varying orientations and is a simplified view of the data not shown here. We then calculated a rank-45 model of the data and for discussion we will focus only on one region of ferrite.

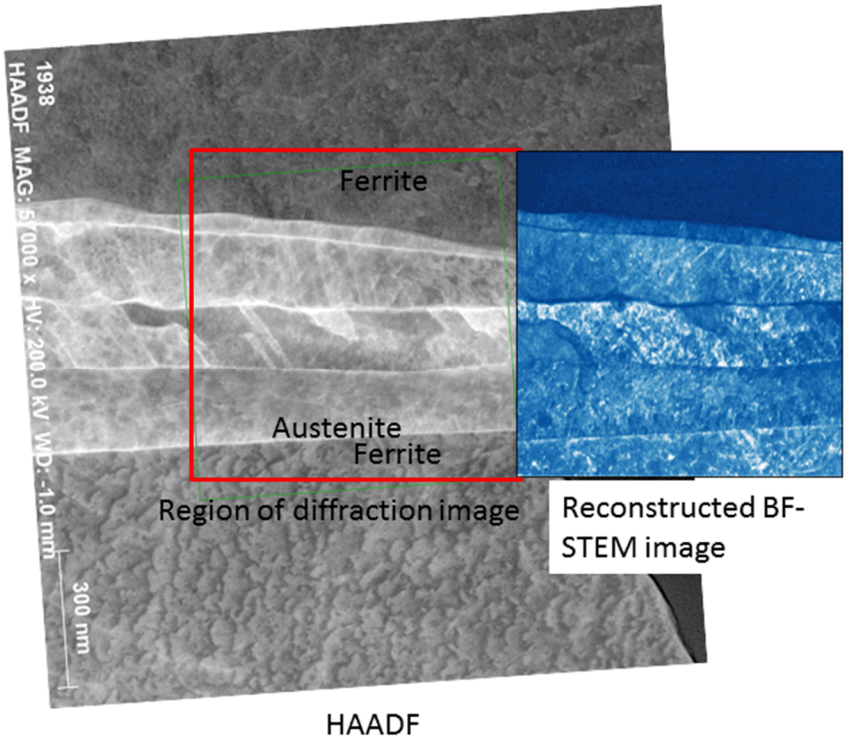

Figure 5. Annular dark-field STEM image. The red box indicates the region from which the diffraction series was acquired and inset to the right is the reconstructed bright-field image.

Figure 5 shows the region from which the diffraction series was acquired. Figure 6 shows a subset of the analysis for the rank-45 model corresponding to the top ferrite region.

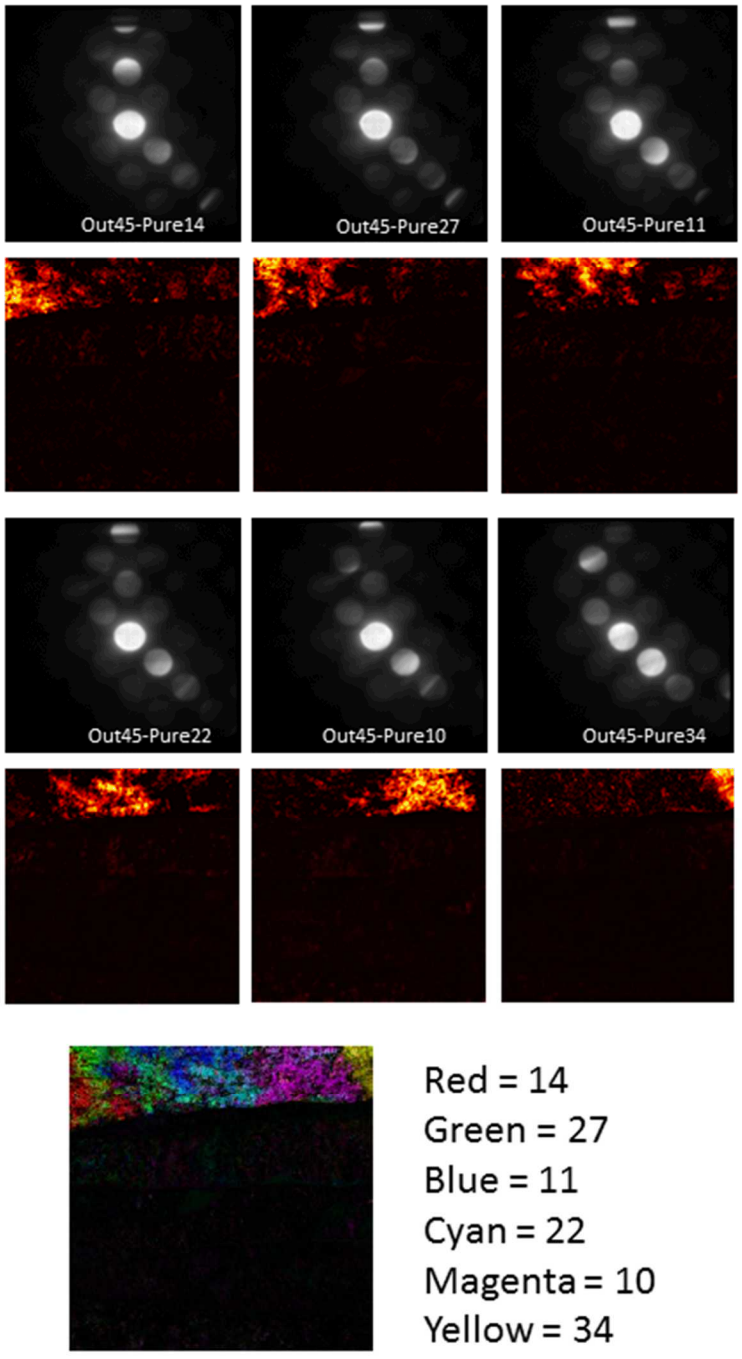

Figure 6. Subset of the rank-45 model from the top ferrite. Corresponding diffraction-space and real-space images for 6 factors corresponding to the ferrite. All look differ by less than a few tenths of a degree change in orientation. Below is a real-space color overlay of the different factors.

Figure 6 shows six of the factors corresponding to the top ferrite region. The difference in the respective diffraction patterns is subtle corresponding in one case to a few hundredths of a degree change in crystallographic orientation with respect to the incident beam. Figure 7 shows two spatially adjacent factors, cyan (#22) and magenta (#10) in the overlay in Figure 6.

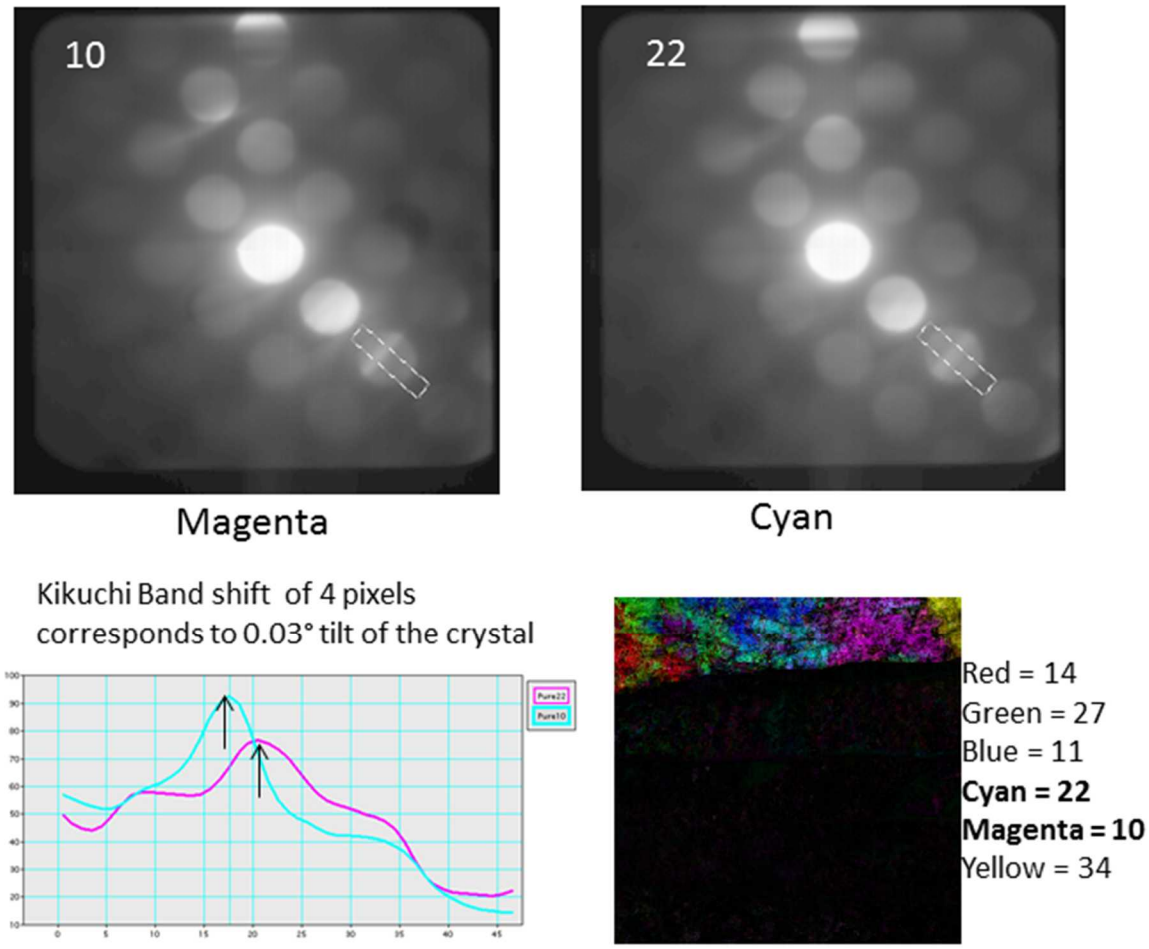

Figure 7. Factors 22 (cyan) and 10 (magenta) and detailed profile of the (022) reflection near the [100] zone axis of the ferrite (bcc). The inset profile across the same respective diffraction indicates a shift of the crossing Kikuchi corresponding to a crystal tilt of 0.03 degrees indicating that the MSA factored results have captured very subtle orientation changes without prior knowledge.

Figure 7 shows a more detailed analysis of two spatially-adjacent factors with a relative crystal tilt of 0.03 degrees indicating the potential sensitivity of the MSA analysis to detect small strains. It is likely that interfacial strain, individual dislocations, and other microstructural features have also been detected but await further analysis.

Conclusions and Future Work

In this small exploratory look at analyzing series of diffraction patterns we have been able to achieve a factor of 100 compression of the PND diffraction series and 100-10,000 for the CBED diffraction data set. We have shown proof of concept that MSA can facilitate the dimensional reduction to make data

interpretation more straightforward. In the case of the CBED data we showed that very small strains can readily bet detected with no a priori knowledge. For aging studies this could allow for rapid analysis of strain at interfaces, phase transformations and other defects with an unbiased approach.

Summary of Findings and Capabilities Related to Aging

No findings relevant to specific component/material aging or capabilities were obtained this year.

References

[1] Kotula, P.G., Keenan, M.R. & Michael, J.R. (2003). *Microsc Microanal* **9**, 1–17.

[2] Brewer, L.N., Kotula, P.G., & Michael, J.R. (2008) *Ultramicroscopy* **108**, 567-578.

[3] Keenan, M.R. (2009) *Surf. Int. Anal.* **41**, 79–87.

[4] Ryll, H., et al., (2013) *Microscopy and Microanalysis* **19** 1160-1161.

[5] Rauch, E.F. & Veron, M. (2005) *Mat.-wiss. u. Werkstofftech.* **36,** 552-556.

Administrative Addendum

H. Ryll, M. Simson, R. Hartmann, P. Holl, M. Huth, S. Ihle, Y. Kondo, **P. Kotula**, A. Liebel, K. Müller-Caspary, A. Rosenauer, R. Sagawa, J. Schmidt, H. Soltau and L. Strüder. "A pnCCD-based, fast direct single electron imaging camera for TEM and STEM," *Journal of Instrumentation* (2016) DOI: 10.1088/1748-0221/11/04/P04006

P.G. Kotula, M.H. Van Benthem, H. Ryll, M. Simson, and H. Soltau. "Multivariate Statistical Analysis of Series of Diffraction Patterns," Presented at Microscopy and Microanalysis 2016, Columbus, OH 24-28 July 2016.

Related Publications and Presentations:

Milestone Status:

Within the first two quarters we will refined the data acquisition methods on both test specimens as well as relevant NW specimens already in our laboratory. By the latter two quarters we showed progress

in developing robust data analysis methods for reducing the raw diffraction data to phase (in concert with X-ray microanalysis) and orientation.

Acronym/Abbreviation List

TEM	Transmission electron microscope
STEM	Scanning TEM
PND	Parallel nano-beam diffraction
CBED	Convergent-beam electron diffraction
MSA	Multivariate statistical analysis

Acknowledgements

Sandia National Laboratories is a multi-mission laboratory managed and operated by Sandia Corporation, a wholly owned subsidiary of Lockheed Martin Corporation, for the U.S. Department of Energy's National Nuclear Security Administration under contract DE-AC04-94AL85000.